Journal of Molecular Structure 1200 (2020) 127034

Contents lists available at ScienceDirect

Journal of Molecular Structure

journal homepage: http://www.elsevier.com/locate/molstruc

Facile synthesis, X-Ray structure of new multi-substituted aryl imidazole ligand, biological screening and DNA binding of its Cr(III), Fe(III) and Cu(II) coordination compounds as potential antibiotic and anticancer drugs

Laila H. Abdel-Rahman [a, *], Antar A. Abdelhamid [a], Ahmed M. Abu-Dief [a], Mohamed R. Shehata [b], Mohamed A. Bakheet [a]

[a] Chemistry Department, Faculty of Science, Sohag University, 82524, Sohag, Egypt
[b] Chemistry Department, Faculty of Science, Cairo University, 12613, Giza, Egypt

ARTICLE INFO

Article history:
Received 24 March 2019
Received in revised form
13 August 2019
Accepted 3 September 2019
Available online 10 September 2019

Keywords:
Aryl imidazole
DNA-binding
Microorganism
Antimicrobial
Anticancer

ABSTRACT

A simple highly adjustable and effective synthesis of aryl imidazole ligand HL namely (2-(1-butyl-4,5-diphenyl-1H-imidazole-2-yl) (4-bromophenol) was discussed where it was prepared by cyclo condensation of 5-bromo-2-hydroxybenzaldehyde, benzil and butan-1-amine. Three new Cr(III), Fe(III) and Cu(II) coordination compounds of aryl imidazole ligand were synthesized. The multi-substituted aryl imidazole ligand (HL) and its coordination compounds were characterized *via* a wide range of spectroscopic and analytical tools such as ^{1}H NMR and ^{13}C NMR, infrared (IR) and UV−Vis spectrophotometry, conductivity and magnetic measurements. The crystal and molecular structure of aryl imidazole ligand HL were discussed by using maXus. The structure of the titled aryl imidazole ligand HL and its metal coordination compounds were discussed theoretically by using Gaussian 09 program at the B3LYP/LANL2DZ level of theory. The obtained data showed that the new compounds have 1:1 M ratio (metal: ligand) and non-electrolytes in nature. The newly prepared $[Cr(L)Cl_2(H_2O)_2]$, $[Fe(L)(NO_3)_2(H_2O)_2]$ and $[Cu(L)Cl(H_2O)_3]$ coordination compounds have a distorted-octahedral geometry. Density Functional Theory (DFT) calculations have been carried out to investigate the equilibrium geometry of the ligands and its coordination compound using Gaussian 09 program at the B3LYP/LANL2DZ level. Moreover, the new compounds were tested against the selected species of microorganism namely *Staphylococcus aureus (+ve), Pseudomonas aeruginosa (-ve), Escherichia coli (-ve)* and also against *Candida albicans*, *Aspergillus flavus* and *Trichophyton Rubrumin*. The result revealed that new compounds showed high efficacy towards the growth inhibition of the selected pathogenic microorganism. Moreover, the interaction of the new coordination compounds with CT-DNA was studied by absorption spectra, gel electrophoresis and viscosity techniques. The result showed that the interaction of the new coordination compounds with CT-DNA is an intercalative binding mode. Furthermore, the growth inhibitory effects of the new compounds were tested against Hep-G2, MCF-7 and HCT-116 cell lines. Moreover, all complexes exhibited stronger cytotoxicity effect on the outgrowth of different types of carcinoma cells, than their corresponding imidazole ligand and follow the order: CuL > CrL > FeL > HL.

1. Introduction

Aryl imidazoles are an important class of heterocycles containing imidazole play an important role in many pharmacological and biological processes [1–4]. Developments in green chemistry and organometallic catalysis have extended the use of imidazoles as N-hetero-cyclic carbenes and ionic liquids [5,6]. Coordination compounds of metal increase the biological activity due to their chelation property with the ligands [7,8]. Imidazole drugs have an expanded field in remedying various arrangements in clinical medicines. Medicinal properties of imidazole involve

* Corresponding author.
E-mail addresses: Laila.abdelrahman@science.sohag.edu.eg, Lailakenawy@hotmail.com (L.H. Abdel-Rahman).

https://doi.org/10.1016/j.molstruc.2019.127034
0022-2860/

anticancer, beta-lactamase inhibitors, carboxy-peptidase inhibitors, heme-oxygenase inhibitors, anti-coagulants, anti-inflammatory, anti-bacterial, anti-fungal, anti-viral, anti-tubercular, anti-diabetic and antimalarial activities [9–13]. A large number of coordination compounds have been studied for their interesting and vital properties such as significant DNA binding ability and anticancer activity, such as, the interaction of Fe(III) and Cu(II) coordination compounds with DNA has been extensively studied in order to develop novel probes of DNA structure, DNA mediated electron transfer reactions and to find the potential biological and pharmaceutical activity. Their activity depends on the mode and affinity of the binding with DNA [14–17]. Furthermore, coordinating compounds of Cu(II) used as cytotoxic agents due to their selective permeability of cancer cell membranes [18,19]. The present work aims to synthesize of aryl imidazole ligand and its new Cr(III), Fe(III) and Cu(II) coordination compounds and to characterize them *via* different spectroscopic and theoretical tools. In addition to that, the anti-microbial bioassays were tested to check their potential activity as new antibiotics and anticancer drugs. The interaction of the newly synthesized coordination compounds with CT-DNA was studied and their binding constants were calculated. From this study, the binding mode of interaction was explained, and the mechanism was suggested.

2. Experimental

The chemical reagents and instruments used in this work are given in the supporting information (S1).

All commercially available reagents were bought from Merck, Aldrich and Fluka. All reactions were checked by thin-layer chromatography (TLC) using percolated plates of silica gel G/UV-254 of 0.25 mm thickness (Merck 60F254) using UV light (254 nm/365 nm) for visualization. Melting points were measured with a Koffler melting points apparatus and uncorrected. Infrared spectra (IR) were recorded with an FT-IR-ALP HBROKER-Platinum-ATR. ^{1}H NMR and ^{13}C NMR spectra were recorded in DMSO-d_6 or $CDCl_3$ on a Bruker Bio Spin AG spectrometer at 400 MHz and 100 MHz, respectively. Elemental analyses were conducted on an elemental analyzer (PerkinElmer 240c) at the main laboratory of Cairo University.

2.1. Synthesis of the new aryl imidazole ligand HL

General procedure for the synthesis of the ionic liquid (piperidinium hydrogen sulphate (PHS), (4.02 g, 0.02 mol) of the aromatic aldehyde (5-bromo-2-hydroxybenzaldehyde), (4.20 g, 0.02 mol) of benzil, (1.54 g, 0.02 mol) of ammonium acetate and (1.46 g, 0.02 mol) of aliphatic amine (Butan-1-amine) were added to (0.5 g, 2.7 mmol) of pyrrolidinium hydrogen sulphate (as green solvent and catalyst). The reaction mixture was stirred for 30–50 min. The reaction mixture was poured into distilled water and filtered. The solid product was crystallized from ethanol to afford pure products. The pure product was obtained without using any chromatographic techniques, simply by recrystallization from ethanol.

For HL ligand: Color: yellow; M. p. 155 °C; yield 95%; FT-IR (KBr, cm^{-1}): 3420 (OH) phenolic, 3071–3048 (C–H) aromatic, 2962–2871 (C–H) aliphatic, 1600 (C=N). ^{1}HNMR ($CDCl_3$-d/D_2O, 400 MHz): δ, 0.84 (t, 3H, $\underline{CH_3}CH_2CH_2CH_2N$), 1.24 (m, 2H, $CH_3\underline{CH_2}CH_2CH_2N$), 1.65 (m, 2H, $CH_3CH_2\underline{CH_2}CH_2N$), 4.04 (t, 2H, $CH_3CH_2CH_2\underline{CH_2}N$), 7.05–7.71 (m, 13H, Ar–H), 12.89 (s. br, 1H, $C_6H_3\underline{OH}$), ^{13}C NMR (100 MHz, $CDCl_3$-d/D_2O): δ = 13.18, 19.48, 32.07, 45.48, 110.37, 119.74, 126.77,127.35, 128.35, 129.33, 129.60,130.15, 131.27, 133.36, 134.35, 143.12, 156.84. Anal. Calc. For $C_{25}H_{23}BrN_2O$: C, 67.12; H, 5.18; N, 6.26. Found (%): C, 67.07; H, 5.17; N, 6.27.

2.2. Synthesis of the new aryl imidazole coordination compounds

(5 mmol, 2.24 g) of the new prepared aryl imidazole ligand HL dissolved in (20 ml) absolute ethanol was added to (5 mmol) of the metal salts in (20 ml) commercial ethanol ($CrCl_3.6H_2O$, $Fe(NO_3)_3.9H_2O$ and $CuCl_2.2H_2O$) (1.33 g, 2.02 g, 0.85 g), respectively in separate flasks. Then, the reaction mixtures were subjected to continuous stirring under reflux at 70 °C for 1 h. The reaction mixtures were filtered to get the different solid products which were crystallized from ethanol to obtain the pure products simply by recrystallization from ethanol (cf. Scheme 1).

$[Cr(L)Cl_2(H_2O)_2]$:FT-IR (KBr, cm^{-1}): 3394 (OH) phenolic, 3071–3048 (C–H) aromatic, 2962–2871 (C–H) aliphatic, 1591 (C=N), 556 (M – O), 439 (M – N).

$[Fe(L)(NO_3)_2(H_2O)_2]$ FT-IR (KBr, cm^{-1}): 3409 (OH) phenolic, 3071–3048 (C–H) aromatic, 2962–2871 (C–H) aliphatic, 1602 (C=N), 567 (M – O), 474 (M – N).

$[Cu(L)Cl(H_2O)_3]$: FT-IR (KBr, cm^{-1}): 3426 (OH) phenolic, 3071–3048 (C–H) aromatic, 2962–2871 (C–H) aliphatic, 1592 (C=N), 519 (M – O), 439 (M – N).

The reported yield, melting point and other physical data of ligand and of coordination compounds were listed in Table 3.

2.3. Estimation of the stoichiometry of the coordination compounds

The estimations of stoichiometry were calculated from the molar ratio and continuous variation methods [20,21]. The mixtures from metals salts and ligand were stirred and allowed to equilibrate. The measured absorbance for each mixture at λ_{max} was plotted against the mole fraction of the ligand or the mole fraction of metal ion. The formation constants (K_f) of the compounds were obtained from spectrophotometric measurements according to the following relation [20,21]:

$$K_f = \frac{\left(\frac{A}{A_m}\right)}{\left(1 - \left(\frac{A}{A_m}\right)^2 C\right.} \quad (1)$$

where A_m is maximum absorbance for each the coordination compounds, A is arbitrarily selected from the values of absorbance on either side of the absorbance peak, and C is the metal concentration. Also, the free energy change of the coordination compound was estimated using the following relation [20,21]:

$$\Delta G^{\neq} = -RTlnK_f \quad (2)$$

2.4. Kinetic studies of prepared coordination compounds

The decomposition and thermal dehydration of the coordination compounds were studied kinetically using the integral method applying the Coats–Redfern method. Moreover, the thermodynamic activation parameters of degradation steps of dehydrated complexes, namely energy of activation (E), frequency factor (A), enthalpy of activation (ΔH), entropy of activation (ΔS) and free energy change of the decomposition (ΔG), were evaluated from TGA data graphically utilizing the Coats–Redfern relation form following equation [22–24]:

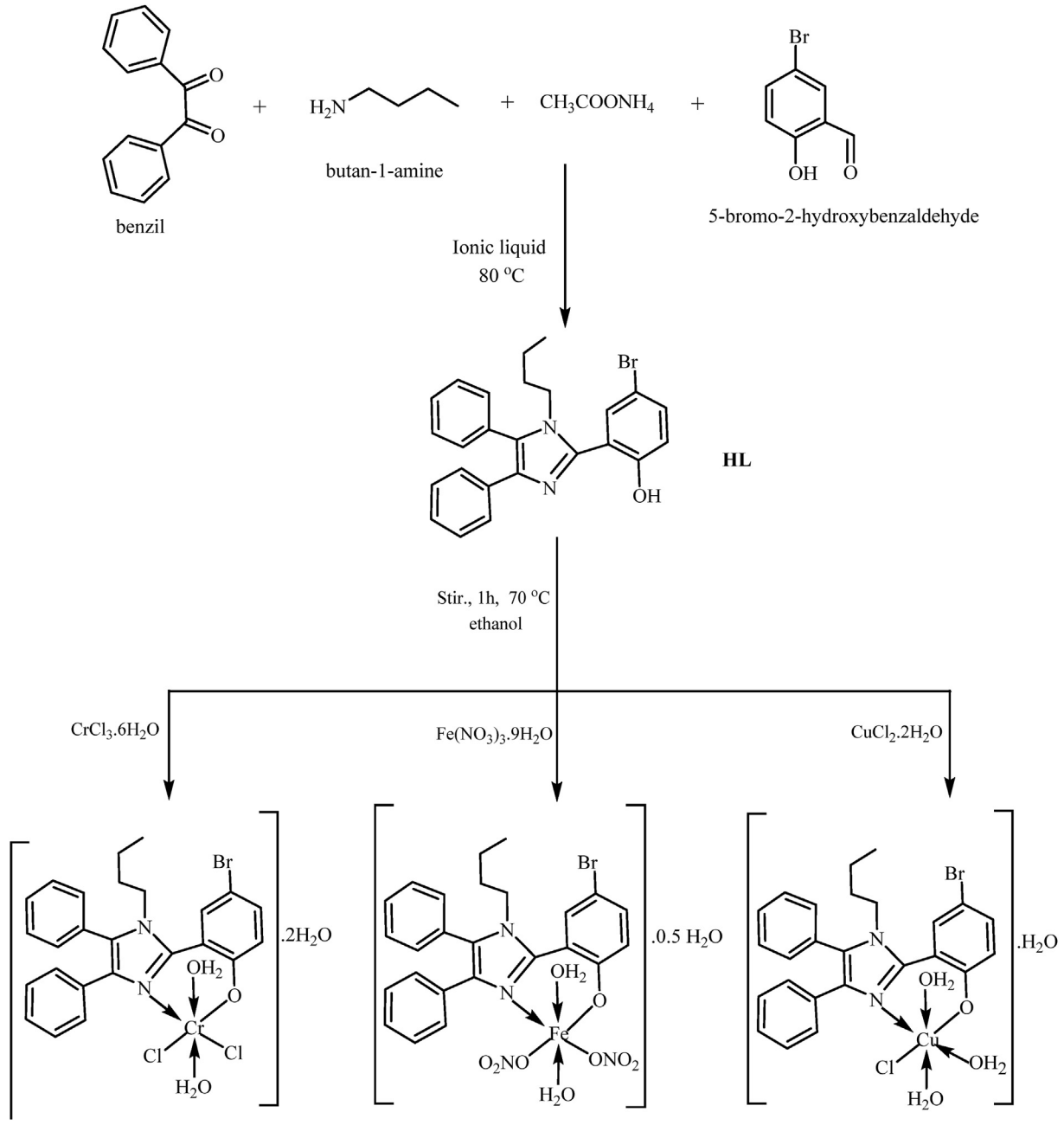

Scheme 1. Synthesis the aryl imidazole ligand HL and its CrL, FeL and CuL compounds.

$$\log\left[\log(w_\infty/(w_\infty - w))\Big/T^2\right] = log\left[\frac{AR}{\varnothing E^*}\left(1 - 2RT/E^{\neq}\right)\right] - \frac{E^{\neq}}{2.303R}\frac{1}{T} \quad (3)$$

where W∞ is the mass loss after the decomposition reaction, W is the cluster loss up to temperature T, R is the general gas constant and ϕ is the heating rate. Since $1 - 2RT/E^* \approx 1$, a plot of the left-hand side of Eq. (1) against 1/T would give a straight line.

E* was calculated from the slope and the Arrhenius constant, A, was determined from the graph intercept. The other kinetic parameters, namely the entropy of activation (ΔS*), enthalpy of activation (ΔH*) and free energy change of activation (ΔG*), were calculated using the following equations:

$$\Delta H^{\neq} = E^{\neq} - RT \quad (4)$$

$$\Delta S^{\neq} = 2.303\mathrm{R}\ \log\left(Ah/k_bT\right) \quad (5)$$

$$\Delta G^{\neq} = \Delta H^{\neq} - T\Delta S \quad (6)$$

where K_b is Boltzmann's constant and h is Planck's constant.

2.5. Crystallographic study of the new HL ligand

Suitable crystals were selected and mounted on glass fiber and data collection was completed for HL on a Bruker APEX

diffractometer with a CCD detector. The structure was solved using maXus program [25]. Crystal data are tabulated below, and full crystallographic tables can be found in the supplementary information.

$C_{25}H_{23}BrN_2OM_r = 447.35$	$V = 4289.1\ (3)Å^3$
Monoclinic	$Z = 8$
C2/c a = 25.0784 (9)Å	$D_x = 1.386$ mg. m^{-3}
b = 8.9263 (3)Å	Mo K_α radiation
c = 20.4607 (11)Å	$\lambda = 0.71073$
$\alpha = 90.00°$	$\mu = 1.935$
$\beta = 110.5387\ (14)°$	T = 298 K
$\gamma = 90.00°$	Cube yellow
	Crystal source: Local laboratory

2.6. Powder XRD patterns

XRD patterns were conducted on PerkinElmer D8 advance, Bruker, Germany, using CuKα1 radiations (1.54060 Å). The operating conditions at the anode are at 30 kV and 15 mA the 2θ angles were measured between 5° and 60° at the rate of 0.02°/min.

2.7. DFT calculation

Density Functional Theory (DFT) calculations have been carried out to investigate the equilibrium geometry of the ligands and coordination compounds using Gaussian 09 program at the B3LYP/LANL2DZ level of theory for the ligand and its coordination compounds [29,30].For the modeling of the ligand the configuration in the experimentally known molecular crystal determined by x-ray, cif file, is used as a starting point for theoretical calculations. For the coordination compounds, different configurations and compositions of coordination's spheres are used and the configurations with the lowest total energy were chosen. Theoretical IR spectra were computed at the same level of the theory to confirm the absence of imaginary frequencies.

2.8. Antimicrobial bioassay

The titled compounds were screened against the selected species of bacteria namely *Staphylococcus aureus (+ve), Pseudomonas aeruginosa (-ve) and Escherichia coli (-ve)*) using agar well dilution method. They were also studied against selected species of fungi namely *Candida albicans*, *Aspergillus flavus* and *Trichophyton Rubrumin* in the well diffusion methods [29–31].The synthesized compounds were dissolved with concentrations 10 and 25 *mg* ml^{-1} in DMSO. Nutrient agar and potato dextrose agar were prepared, then sterilized in an autoclave, poured in sterile Petri plates, separately and left to cool. Then the studied bacteria and fungi strains were grown on nutrient agar and potato dextrose agar, respectively. After that, the sterile Paper discs of Whatman saturated with the solution of the prepared compounds were placed in the agar using a sterile crook borer for working holes. They were incubated for 24 h at 37 °C for bacteria strains and 72 h at 35 °C for fungi strains. For comparison, the tetracycline drug (standard antibacterial) and fluconazole (standard antifungal) were tested under the same conditions. The inhibition zone around each sample of free ligand, metal salt and the coordination compounds were done in triplicates for each species of bacteria and fungi.

2.9. CT-DNA binding of the new coordination compounds

CT-DNA was dissolved in Tris–HCl buffer with concentration 60 mM in pH = 7.2 and stored at 4 °C. The prepared coordination compounds were dissolved in acetonitrile solvent.

2.9.1. Electronic spectra

Electronic spectra experiments were carried out with fixing coordination compounds concentrations and changing the CT-DNA concentration in the interaction medium. From the electronic spectra data, the intrinsic binding constant (K_b) was calculated according to the following relation [29–32]:

$$[DNA]\Big/\left(\varepsilon_a - \varepsilon_f\right) = [DNA]\frac{1}{\left(\varepsilon_b - \varepsilon_f\right)} + \frac{1}{K_b}\frac{1}{\left[\left(\varepsilon_b - \varepsilon_f\right)\right]} \tag{7}$$

where [DNA] is the molar CT-DNA concentration and base pairs ε_f, ε_a and ε_b are the extinction coefficients of free, apparent and fully bound coordination compound, respectively. The standard Gibbs free energy ($\Delta G_b^{\neq}$) was determined from the following equation [29–32]:

$$\Delta G_b^{\neq} = -RT\ lin K_b \tag{8}$$

2.9.2. Viscosity measurements

Oswald micro-viscometer was used to determine the viscosity of CT-DNA with the newly prepared coordination compounds. With maintaining the concentration of CT-DNA constant (400 μ M), the fluidity times were registered for different concentrations of the new coordination compounds (0–250 μ M). η^o is the relative viscosities for the CT-DNA with newly prepared coordination compounds and determined from the following relation [29–32]:

$$\eta = (t - t^{\circ})/t^{\circ} \tag{9}$$

2.9.3. Gel electrophoresis

The gel electrophoresis is used as a method for studying the binding coordination compounds with DNA. The coordination compound added to CT-DNA in equal volume and incubated at 37 °C for 1 h. After that, the mixtures were mixed with DNA Loading Dye at a 1:1 M ratio and then loaded onto the wells gel (1%) in TBE buffer. Then a constant voltage (100 V) was applied for 60 min. Finally, the gel has been imagined under UV light using the trans-illuminator. Panasonic DMC-LZ5 Lumix DNA gel documentation is used for photographing the illuminated gel [29–31].

2.10. Anticancer activity

The prepared compounds were screened for their anticancer efficacy against Hep-G2 cell line, MCF-7 cell line and HCT-116 cell line at Cairo University, Cancer Biology Department and the National Cancer Institute. The absorbance was estimated with an ELISA microplate reader (Σ960, Meter Tech, USA) at 564 nm. Firstly, in a 96-multiwell plate, Cells were placed (104 cells per well) at 37 °C for 24 h. Secondly, different concentrations of the new compounds (0–10 μM) were added to this plat and then incubated at 37 °C for 48 h in an atmosphere of 5% CO_2. Then it was fixed, rinsed and stained with sulforhodamine B stain. Acetic acid is used to remove excess stain and then this plate was treated with Tris–EDTA buffer. The inhibition concentration percent (IC_{50}%) was calculated from the following equation [29–31]:

$$IC_{50}(\%) = \frac{control_{\ OD} - compound_{\ OD}}{control_{\ OD}} \times 100 \tag{10}$$

3. Results and discussion

3.1. Elemental analyses and electrical conductivity measurements

All the prepared coordination compounds are solid, stable at room temperature and variegated. The elemental analyses results suggested that the aryl imidazole ligand HL acts as a bidentate ligand and coordinates to Cr(III), Fe(III) and Cu(II) ions in 1:1 M ratio to form the compounds $[Cr(L)Cl_2(H_2O)_2]$, $[Fe(L)(NO_3)_2(H_2O)_2]$ and $[Cu(L)Cl(H_2O)_3]$, respectively (cf. Table 3). The molar conductance of all prepared compounds was measured for 1×10^{-3} mol L^{-1} at room temperature in DMF as a solvent and these values within the range 6.71–9.37 Ω^{-1} cm^2 mol^{-1} which evidences their non-electrolytic behavior (cf. Table 3) [26–31]. Moreover, the Kohlrausch curves for the new compounds were plotted to study their electrochemical behavior (cf. Fig. S1). The variation in conductivity values for different concentration of the prepared compounds could be ascribed to the polarization of the compounds and ligands exchange in solution and partial electrolytic character of DMF solution.

3.2. Infrared spectroscopy

The IR characteristic frequencies for the aryl imidazole ligand HL and its coordination compounds were listed in Table 1 and showed in Fig. 1. The appearance of bands characteristic for –OH and –C═N groups are special and show proof regarding the ligand structure and its bonding with different metals. The IR spectrum of the ligand HL shows bands in the region 3420 and 1600 cm^{-1} indicating to –OH and –C═N groups, respectively. Upon coordination, the disappearance of –OH group band was observed which could be referred to as the participation of –OH group in coordination compound formation and this is further supported by the appearance M – O new band in IR spectra of all coordination compounds [30]. Also, the change of –C═N band position indicates that –C═N group coordinate with different metal ions to form coordination compounds. This is supported by the appearance of a new M – N band in the IR spectra of the new coordination compounds (cf. Figs. 1, S2 and S3). The newly prepared coordination compounds also have coordinated water molecules which were proven by the appearance of bands in the region 3394-3426 $cm^{-1}$and further confirmed from thermal analysis results.

Table 1
Characteristic IR bands (cm^{-1}) of the aryl imidazole ligand HL and its coordination compounds.

Compounds	ν(OH)/H_2O	ν(C═N)	ν (C–O)	ν (M – O)	ν (M – N)
HL	3420	1600	1253	–	–
CrL	3394	1592	1255	556	439
FeL	3409	1612	1252	557	474
CuL	3426	1602	1254	519	439

3.3. ^1H NMR and ^{13}C NMR spectra

In the ^1H NMR spectrum of HL ligand (cf. Fig. S4), a signal of OH proton appears at 12.89 ppm. The aliphatic protons resonate in the region 0.84–4.04 ppm. In addition to that, the aromatic protons appear in the region 7.05–7.71 ppm. The ^{13}C NMR spectrum (cf. Fig. S5), –C═N group shows a singlet signal at 156.84 MHz. The aliphatic signals appeared at 13.18, 19.48, 32.07, 45.48 which are corresponding to (CH_3–CH_2–CH_2–CH_2–N), and the aromatic rings appear in the region 110.17–143.12 MHz, respectively.

3.4. Electronic spectroscopy

The electronic spectra have assured the stereochemistry of metal ions in the coordination compounds structure based on the sites and number of d–d transition peaks [29–32]. The values of the molar absorptivity (ε_{max}) and the maximum absorption wavelength (λ_{max}) are recorded in Table 2 and displayed in Fig. 2. The electronic spectra of aryl imidazole ligand and its coordination compounds are showed in the wavelength range 200–800 nm and at 298 K n → π* transition of the ligand HL appears around λ_{max} = 270 nm. Charge transfer within the aryl imidazole ligand HL to the metal ion appears around λ_{max} = 288, 355 and 291 nm in the absorption bands of CrL, CuL and FeL, respectively. d → d transitions in the structure of CrL, CuL, and FeL appear in the region 439–474 nm.

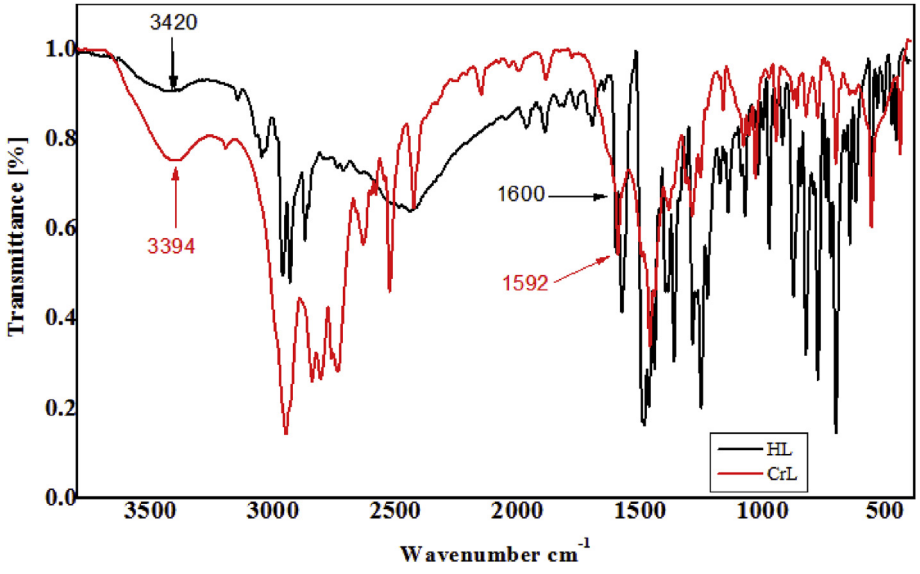

Fig. 1. IR spectrum of the ligand HL and its CrL coordination compound.

Table 2
The electronic spectral parameters at λ_{max} (nm) of the ligand HL and its coordination compounds in acetonitrile.

v	Concentration/mol L^{-1}	$\pi \rightarrow \pi^*$	$n \rightarrow \pi^*$	Intra ligand band	LMCT band	d-d band
HL	1 X 10^{-3}	239	251 270	288	–	–
CrL	1 X 10^{-3}	239	252	270	288	437
FeL	1 X 10^{-3}	239	–	287	291	415
CuL	1 X 10^{-3}	239 251	270	290	355	421

Table 3
Physical, analytical data, formation constant values (K_f), the stability constant (pK) and Gibbs free energy ($\Delta G^{\neq}$) for of the ligand HL and its prepared compounds.

Compound (Molecular formula)	Color	Yield (%)	Molecular weight	M.p. (°C)	Λm (Ω-1cm^2 Mol^{-1})	μeff (B. M)	Analysis (%) Found (calc.)			Type	$K_f \times 10^6$	pK	ΔG^* (kJ mol^{-1})
							C	H	N				
HL ($C_{25}H_{23}BrN_2O$)	yellow	95	447	155	–	–	67.07 (67.12)	5.17 (5.18)	6.27 (6.26)				
CrL ($C_{25}H_{30}N_2O_5BrCl_2Cr$)	Green	68	641	220	7.53	3.12	46.71 (46.80)	4.61 (4.68)	4.41 (4.36)	1:1	13.3	16.4	40.6
FeL ($C_{25}H_{27}N_4O_{9.5}BrFe$)	Red	67	671	180	9.37	2.89	44.73 (44.65)	3.95 (4.02)	8.40 (8.33)	1:1	19.0	16.8	41.6
CuL ($C_{25}H_{30}N_2O_5BrClCu$)	DarkGreen	70	617	170	6.71	1.74	48.70 (48.62)	4.80 (4.86)	4.60 (4.53)	1:1	11.5	16.3	40.4

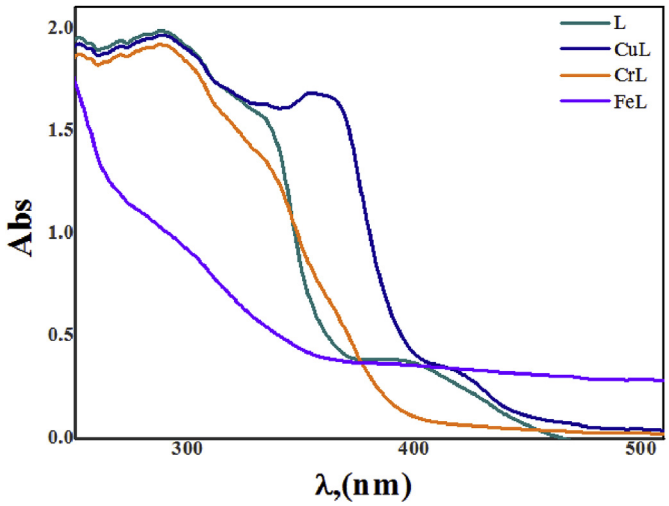

Fig. 2. Electronic spectra of the synthesized aryl imidazole ligand and its coordinationcompounds in acetonitrile with concentration 10^{-3} M at 298 K.

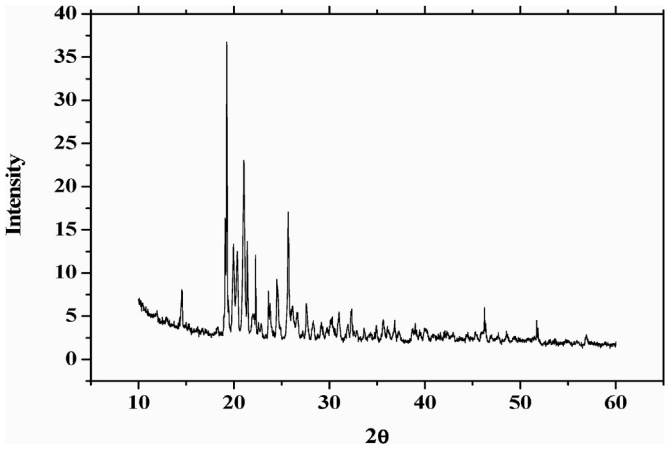

Fig. 3. XRD powder pattern of $[Cu(L)Cl(H_2O)_3]$ coordination compound.

3.5. Powder XRD of the prepared compounds

XRD diffraction pattern for the prepared coordination compounds, together with the corresponding ligand are graphically presented in Fig. S6. Here, we focus only on presenting the XRD patterns obtained for the coordination compound (CuL). The particle size of the sample is estimated using Scherrer's formula. According to Scherrer's equation, the particle size is given by $t = 0.9\,\lambda / B\cos\theta$, where t is the crystal thickness (in nm), B is half-width (in radians),θ is the Bragg angle and λ is the wavelength. The particle size corresponding to each diffraction maxima is determined from the measurement of the half-width of the diffraction peak. The particle size was found to be 52 nm for the complex. The XRD pattern is indicative of the crystalline nature of the CuL compound which is confirmed by the main peaks positioned. X-ray analysis reveals that the sample is monoclinic in phase as shown in Fig. 3.

3.6. Spectrophotometric determination of the stoichiometry of the new coordination compounds

3.6.1. Continuous variations and molar ratio methods

Continuous variation and molar ratio are methods used for estimating the stoichiometry of the coordination compounds [33–36].The continuous variation curve displays absorbance maximum at mole fraction X ligand = 0.48–0.51and this indicated that the prepared coordination compounds are presented in (1:1) metal: ligand (cf. Fig. S7). The molar ratio curves confirm the obtained results from continuous variation curves (cf. Fig. S8). The obtained K_f values indicated that the titled coordination compounds have high stability (cf. Table 3). The reaction is spontaneous and favored as showing from the negative values of Gibbs free energy [29–31].

3.7. Magnetic measurements

The magnetic susceptibility measurements give information considering the geometric structure of the compounds. The

recorded magnetic moments of the prepared coordination compounds are generally diagnostic of the coordination geometry around the metal ion (cf. Table 3). Magnetic susceptibility measurements indicated that the prepared compounds CrL, FeL and CuL are paramagnetic and have distorted octahedral geometries [29,32].

3.8. Thermal gravimetric analysis

Thermal gravimetric analysis was used to evaluate the thermal stability of the coordination compounds and confirm the existence of hydrated and coordinated water molecules in the structure of the coordination compounds [30]. In the case of CrL compound, the thermogram shows five degradation steps within the temperature range 30–605 °C (cf. Table S1)(see Scheme 2). The first stage at 30–110 °C assigns to the loss of two hydrated water molecules. The second step at 115–205 °C assigns to the loss of two coordinated water molecules. The third stage at 205–360 °C assigns to the loss of Cl^- ions. The fourth stage at 362–480 °C refers to the loss C_6H_3Br molecule. The fifth stage at 481–605 °C assigns to the loss $C_{19}H_{19}N_2$ molecule to give 1/2 Cr_2O_3 as a residue. In FeL compound, the thermal analysis curve displays four degradation steps within the temperature range of 37–615 °C (cf. Table S1). The first weight loss at the range 37–200 °C corresponds to the removal of one hydrated and two coordinated water molecules. The second step at 200–380 °C and could be assigned to the removal of $2NO_3$ groups. The third step occurred at a temperature range 380–480 °C and could be referred to as the loss C_6H_3Br fragment of the ligand. The fourth weight loss was displayed at the range 480–615 °C and assigned to the loss $C_{19}H_{19}N_2$ fragment. The final remaining residue was 1/2 Fe_2O_3. In CuL, the thermogram shows five degradation steps within the temperature range 35–610 °C to give CuO as the final product [36,37]. (cf. Table S1). The released organic molecules (e.g. C_6H_3Br moiety) for the prepared compounds were proven by IR spectra, the coordination compounds were heated until 350 °C and measured ex-situ at room temperature.

3.8.1. Kinetic parameter for TGA of the new coordination compounds

The energy of activation ($E^{\pm}$), Arrhenius constant (A), the entropy of activation ($\Delta S^{\pm}$), the enthalpy of activation ($H^{\pm}$) and the free energy change ($\Delta G^{\pm}$) were recorded in Table S1. The $\Delta S^{\pm}$ values are negative indicating that the coordination compounds are more activate than the ligand and so the degradation processes are unfavorable [38]. The $H^{\pm}$ values are positive indicating that degradation processes are exothermic. It is indicated that $G^{\pm}$ values increase with increasing temperature [39]. There is a direct relation between ($E^{\neq}$) and (A) for the obtained coordination compounds. The relative low values of (A) showed that the nature of the pyrolysis reaction is slow. The greater positive values of ($E^{\neq}$) showed that the processes involve translational, vibrational states and changes in mechanical potential energy for the prepared coordination compound [40].

3.9. Stability range of the coordination compounds

The pH curves show a high stability range of pH (5–11) of the synthesized coordination compounds (Fig. S9). The synthesized coordination compounds are more stable than their ligand HL [41].

3.10. Crystal and molecular structure

Crystals of the aryl imidazole ligand HL suitable for X-ray diffraction were grown from slow evaporation of ethanol. The free base crystallizes in the monoclinic C2/c space group. Fig. 4a and b shows the ORTEP diagram with the atomic numbering scheme and close packing structure for HL aryl imidazole ligand. Selected bond lengths (Å) and angles (°) for HL are listed in Table S2. The unit cell contains eight molecules per unit cell with intermolecular hydrogen bonds between O–H and N2, where N2 ···· H is longer in x-ray data than those obtained out of DFT calculations. The bond lengths and angles of ligand (HL) obtained from x-ray results and DFT calculations are compared very well (Table S2).

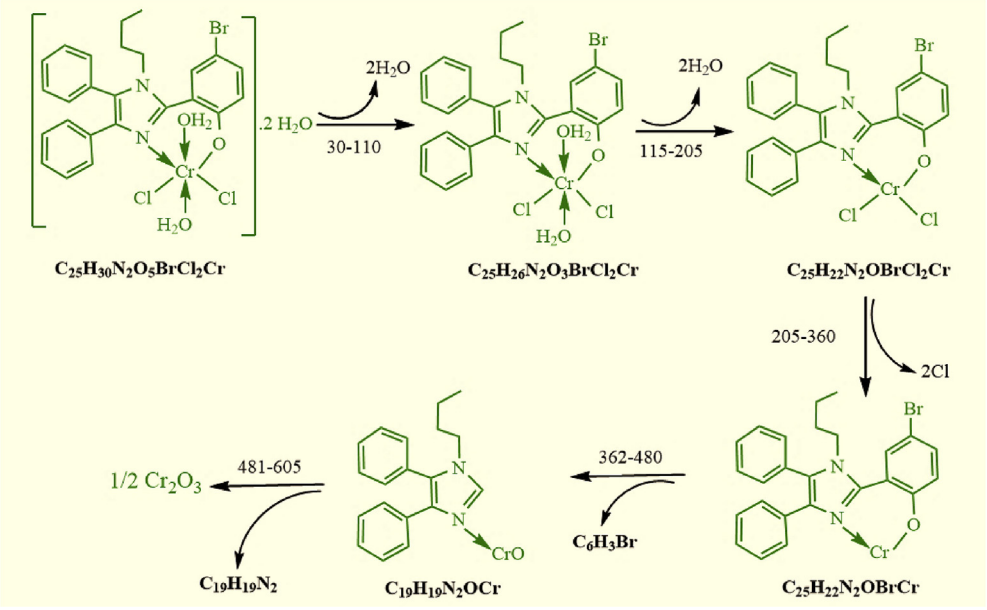

Scheme 2. Thermal degradation steps of CrL compound.

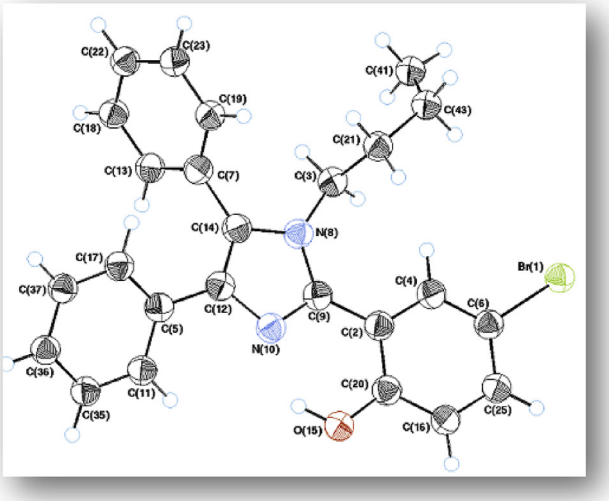

a

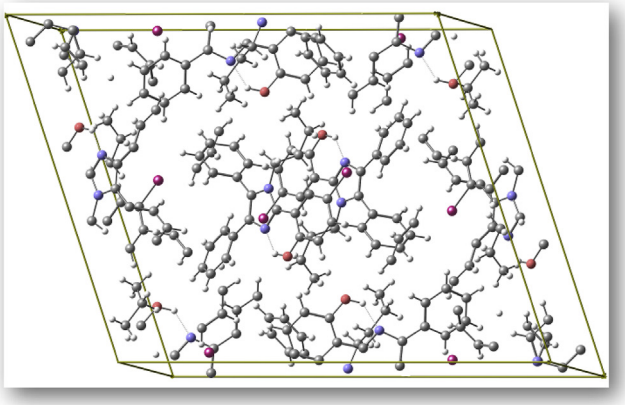

b

Fig. 4. a: ORTEP structure of Ligand HL showing 50% probability ellipsoids. **b**. Unit cell drawing of Ligand (HL), showing eight molecules per unit cell.

3.11. Molecular DFT calculations

3.11.1. Molecular DFT calculation of ligand HL

Fig. S10 shows the optimized structures of HL as the lowest energy configurations. The Chelpg charges obtained from a method developed by Breneman and Wiberg show that the more negative active sites are in order O1 (−0.728) > N2 (−0.555) > N1 (−0.265). This indicated that the metal ions prefer bidentate coordination to O1 and N2 forming a 5-membered ring.

3.11.2. Molecular DFT calculation of $[Cr(L)Cl_2(H_2O)_2]$

Fig. S11 shows the optimized structures of the coordination compound $[Cr(L)Cl_2(H_2O)_2]$ as the lowest energy configurations. The chromium atom is six-coordinate in a distorted-octahedral geometry with O2 and O3 of water molecules are in axial position and atoms O1, N2, *Cl*2 and *Cl*1 are almost in one plane deviated by 0.479°. The bite angle O1—Cr—N2 (83.81°) is lower than 90° due to chelation. The bond angles in the octahedral geometry are ranging from 82.73° to 101.9° (cf. Table S3). The Chelpg charges, obtained from a method developed by Breneman and Wiberg, on the coordinated atoms are Cr (+1.013), O1 (−0.622), N2 (−0.211), O2 (−0.863), O3 (−0.915), *Cl*1 (−0.557) and *Cl*2 (−0.542) (Fig. S11).

3.11.3. Molecular modeling of $[Fe(L)(NO_3)_2(H_2O)_2]$

Fig. S12 shows the optimized structures of the coordination compound $[Fe(L)(NO_3)_2(H_2O)_2]$ as the most stable configurations. The iron atom is six-coordinate in a distorted-octahedral geometry, the bond angles ranging from 80.41° to 96.01° (cf. Table S4). The iron atom is six-coordinate in a distorted-octahedral geometry with O4 and O5 of water molecules are in axial position and atoms N1, O1, O2 and O3 are exactly in one plane. The water molecule H23—O4—H24 makes two H-bonds with O6 and O9 of nitrate groups, consequently, longer bond lengths of O4—H23 (1.004 Å) and O4—H23 (1.001 Å) compared to O5—H25 (0.982 Å) and O5—H26 (0.984 Å), Table S4. The Chelpg charges, obtained from a method developed by Breneman and Wiberg, on the coordinated atoms are Fe (+1.334), O1 (−0.632), N2 (−0.308), O2 (−0.660), O3 (−0.692), O4 (−1.081) and O5 (−1.036) (Fig. S12).

3.11.4. Molecular DFT calculation of $[Cu(L)Cl(H_2O)_3]$

Figs. S13—a shows the optimized structures of the coordination compound $[Cu(L)Cl(H_2O)_3]$ as the lowest energy configurations. The copper atom is six-coordinate in a distorted-octahedral geometry with O3 and O4 of water molecules are in axial position. The dihedral angle of atoms in the plane O1, O3, O2 and O4 is −0.141°, indicates that these atoms are almost in one plane. The bond angles in the octahedral geometry are ranging from 73.42° to 102.1° (Table S5). The Chelpg charges, obtained from a method developed by Breneman and Wiberg, on the coordinated atoms are Cu (+1.047), O1 (−0.768), N2 (−0.324), O2 (−0.910), O3 (−0.891), O4 (−1.045) and *Cl* (−0.624).

Figs. S13—b shows the optimized structures of the four possible isomers of coordination compound $[Cu(L)Cl(H_2O)_3]$ as the lowest energy configurations. The total energy of structure (I), −1604.128 Hartree = −4211637.7 kJ/mol < structure (II), −1604.116 Hartree = −4211606.2 kJ/mol < structure (III), 1604.078 Hartree = −4211506.4 kJ/mol < structure (IV) 1604.055 Hartree = −4211446.0 kJ/mol). The structure I, is more negative by 31.5 kJ/mol than Structure II. So, the total energy in the case of structure I (where the chorine atom is trans to N2 has the lowest energy of the four possible isomers (Figs. S13—b).

Similar results were obtained for Cr(III) and Fe(III) coordination compounds, where six possible isomers for each case, (Fig. S11-b and S12-b). In the case of $[Cr(L)Cl_2(H_2O)_2]$ structure, I with two water molecules coordinated trans is the most stable lowest energy structure (Figs. S11—b). In the case of $[Fe(L)(NO_3)_2(H_2O)_2]$ structure, I with two water molecules coordinated trans is the most stable lowest energy structure (Figs. S12—b).

The computed total energy, the highest occupied molecular orbital (HOMO) energies, the lowest unoccupied molecular orbital (LUMO) energies and the dipole moments for the ligands and coordination compounds were listed in Table S6. The more negative values of the total energy of the coordination compound than those of free ligands indicate that the coordination compounds are more stable than the free ligands. Also, the energy gaps (E_g) = E_{LUMO} - E_{HOMO} are smaller in the case of coordination compound than that of ligand due to the chelation of ligand to metal ions. The polarity of the coordination compounds is much larger than the free ligand (cf. Table S6).

3.12. Antimicrobial bioassay

The principal aim of any antimicrobial compound is to inhibit microbial activity without any side effects to patients. Overall, this activity is enhanced by complexing with metal, but it is also

influenced by its nature and coordination mode. The biological activity of the metal compounds depends on the following factors:

i. The chelate effect of the ligands.
ii. The total charge on the complex ion.
iii. The nature of the donor atoms.
iv. The nature of the counter ions that neutralize the complex.
v. The nature of the metal ion.
vi. The geometrical structure of the complex.

The increased activity of the metal chelates can be explained based on chelation theory [42–44]. According to the concept of cell permeability, the lipid membrane surrounding a cell favors the passage of only lipid-soluble materials since lipid solubility is considered to be an important factor that controls antimicrobial activity. On chelation, the polarity of the metal ion will be reduced to a greater extent due to the partial sharing of the positive charge of metal ions with donor groups and the overlap of the ligand orbital. Furthermore, it increases the delocalization of the electrons over the whole chelate ring and enhances the lipophilicity of the complex. This increased lipophilicity enhances the penetration of the complexes into the lipid membrane which can then block the metal-binding sites on enzymes of microorganisms. These metal complexes also disturb the respiration process of the cell and thus block the synthesis of proteins, which restricts further growth of the organism. The variation in the activity of different coordination compounds against different organisms depends either on the impermeability of microbe cells or difference in microbe ribosomes.

The aryl imidazole compounds involve three different metals, chrome, iron and copper, having NO coordination. The aryl imidazole ligand and its coordination compounds were screened for antimicrobial activity in DMSO solvent as a control substance. Furthermore, the antibacterial activity of these compounds was also compared with that of commercial antibiotics, namely tetracycline, and the antifungal activity was compared with that of fluconazole. All the synthesized compounds exhibited varying degrees of inhibitory effects on the growth of different test strains. In general, the coordination compounds are more potent bactericides than the ligand and its metal salts. The antibacterial screening results exhibited marked enhancement of activity in coordination with the metal ions against test bacterial strains. It has also been suggested that ligands with nitrogen and oxygen donor systems might inhibit enzyme production since the enzymes which require these groups for their activity appear to be especially susceptible to deactivation by the metal ions upon chelation [45]. So the enhanced activities of the metal chelates compared to the free ligand may be attributed to the increase in the number of oxygen groups around the central metal atom arising from chelation, and hence the central metal atom was not only responsible for biological activity because some metal chelates can enhance activity and others can reduce activity with respect to the parent ligand [46]. The orbital of each metal ion is made to overlap with the ligand orbital. Increased activity enhances the lipophilicity of complexes due to the delocalization of π - electrons in the chelate ring [47]. In some cases increased lipophilicity leads to the breakdown of the permeability barrier of the cell [42,48–51]. The antibacterial and antifungal activity of HL, its compounds and the metal salts were studied against different bacterial strains namely *Escherichia coli (-ve), Staphylococcus aureus (+ve)* and *Pseudomonas aeruginosa (-ve)* and also against fungi strains namely *Candida albicans, Aspergillus flavus and Trichophyton Rubrumin* [23–26]. The results are summarized in Tables S7 and S8 and shown in Fig. 5, S14 and S15.

The potency index of the titled imidazole ligand HL, metal salts and its coordination compounds were calculated according to the following relation [29–31]:

$$\text{Activity index} = \frac{\textit{Inhibition zone of compound (mm)}}{\textit{Inhibition zone of the standard drug (mm)}} \times 100 \quad (11)$$

Minimum inhibition concentrations (MIC) values of the studied imidazole ligand HL and its coordination compounds against selected microorganisms are listed in Table S10. The antimicrobial screening data show that the newly prepared coordination compounds have a greater inhibitory effect than the free ligand and the metal salts (cf. Table S9). From the obtained results it is clear that the biocidal activity of the new compounds against gram-positive and gram-negative bacteria follow the order: Tetracycline > CuL > CrL > FeL > HL. On comparing the biological activity of the new compounds with those in literature [54–56], we found that the prepared coordination compounds are more active than those shown in Table S11.

3.13. CT-DNA binding assay of the new coordination compounds

The interaction of metal complexes with DNA is essential to the development of anticancer drugs [58].

3.13.1. Electronic spectroscopy of the CT-DNA binding

Electronic spectroscopy is a method to study the binding metals coordination compound with CT-DNA [28–32]. The absorption spectra of interaction the titled coordination compounds with CT-DNA are displayed in Figs. S16, S17 and S18. The curves indicated that there is a significant hypochromic red-shift peak in the electronic spectra of the prepared coordination compound so the interaction mode is intercalation [28–31,52,53]. This is due to the strong $\pi \rightarrow \pi^*$ transition which occurred after the stacking interaction between the aromatic chromophore imidazole ligand of the coordination compound and the base pairs of CT-DNA. The spectroscopic parameters and K_b for the interaction of the synthesized coordination compound with CT-DNA are recorded in Table S12. The order of titled coordination compounds according to the K_b values is CuL < CrL < FeL (cf. Figs. S19–S21).

3.13.2. Viscosity measurements

Viscosity, which is very sensitive to molecular length increase, is considered as one of the least ambiguous and most critical tests for exploring the bonding mode of coordination compounds with DNA [28–31,57,58]. Viscosity measurements were used to further elucidate the nature of the interactions between the coordination compounds and DNA. A classical intercalator causes a significant increase in the viscosity of DNA solution due to increased separation of the base pairs increasing overall DNA length, whereas partial or non-classical intercalation of coordination compounds may bend the DNA helix, resulting in a decrease in its effective length and a concomitant decrease in viscosity. The effects of the aryl imidazole coordination compounds on the viscosity of DNA solutions are shown in Fig. S22. As seen, the relative viscosity of DNA is increased in the presence of coordination compounds CrL, FeL and CuL relative to ethidium bromide, indicating intercalative binding mode [28–31,59–61]. These viscosity results are consistent with the spectroscopic results discussed above.

3.13.3. Gel electrophoresis

The gel electrophoresis technique is used to investigate the binding of the new compounds with DNA Gel electrophoresis pictures are shown in Fig. S23. The photograph compares the bands

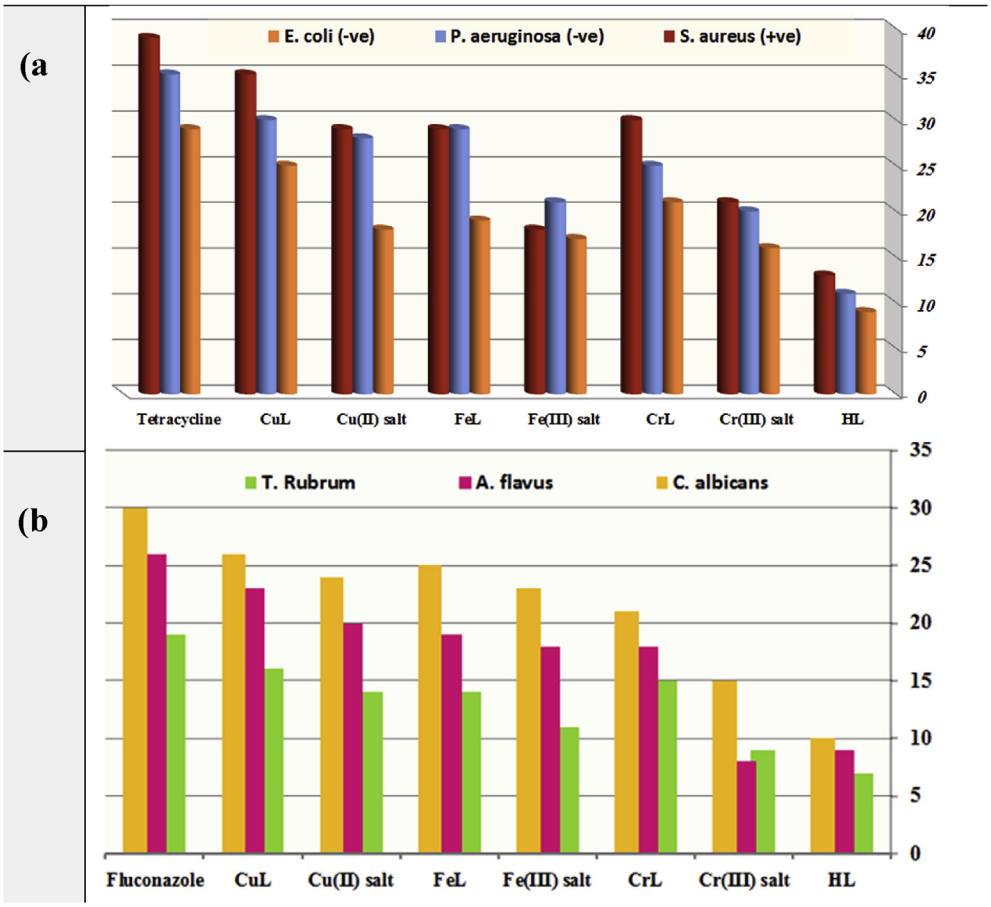

Fig. 5. Graph showing the comparative **a)** antibacterial **b)** antifungal bioassay of the aryl imidazole Ligand HL, metal salts and the new compounds at concentration of 25 mg ml^{-1}.

with different bandwidths and brightness tithe control. The diversity in DNA—cleavage efficiency of the new coordination compounds was attributed to their difference in the binding ability to DNA. It was concluded that when the coordination compounds cleaved DNA, the pathogenic growth was arrested through the destruction of the genome of the organism [62].

3.14. Anticancer activity

Metal-based anticancer drug discovery is one of the advanced areas of pharmaceutical research. The anticancer activity of the prepared aryl imidazole ligand HL and its Cr(III), Fe(III) and Cu(II) coordination compounds was determined against breast carcinoma (MCF-7 cell line), human hepatic cellular carcinoma (HepG-2) and colon carcinoma (HCT-116) cell line using vinblastine as a reference drug control (cf. Table S13 and Fig. 6).

The IC_{50} (the concentration of the compound in μg/ml that inhibits proliferation of the cells by 50% as compared to the untreated control cells) values of the new compounds against human breast cancer cell lines were ranged from 10.5 to 40.24 μg/ml. The IC_{50} value of CuL compound is 10.5 μg/ml towards human breast cancer cell lines (MCF-7), while the standard drug vinblastine exhibited with IC_{50} value 5.71 μg/ml. The tested compounds were also exhibited good anticancer activity against hepatocellular carcinoma (Hep-G2 cell line)with IC_{50} values of 20.24—40.47 μg/ml. The least activity was observed for colon carcinoma (HCT-116 cell line) which gave IC_{50} values from 28.1 to 65.47 μg/ml. The cytotoxic activity of the aryl imidazole ligand and its compounds against hepatocellular carcinoma (Hep-G2 cell line), breast carcinoma (MCF-7 cell line) and colon carcinoma (HCT-116 cell line) follows the order: MCF-7>Hep-G2>HCT-116. Regarding selectivity, the prepared aryl imidazole compounds have a positive impact against all cancer cell lines, and in all cases, the impact was higher than that of their subsequent aryl imidazole ligand. This outcome indicated that the chelation of aryl imidazole ligand with Cr(III), Fe(III) and Cu(II) metal ions was critical for the activity of these novel compounds considering the Tweedy's chelation theory [28—31,63,64]. The nature of the metal ions and the type of ligand has an impact on the cytotoxicity of the compounds. The cytotoxic potency may be explained in that the positive charge of the metal increases the acidity of coordinated pro-ligands that gives protons, causing more potent hydrogen bonds that enhance the biological activity [65,66]. The order of the IC_{50} for the MCF-7, HepG-2 and HCT-116 can be arranged as follows: Cu(II) < Cr(III) <Fe(III) < HL. Moreover, it has been found that complex CuL showed the most powerful anticancer effect with an IC_{50} value of 10.5 μg/ml against breast carcinoma (MCF-7 cell line), which was significant and comparable to that of the reference drug vinblastine IC_{50} value of 5.71 μg/ml Table S13. These observations reflect the effect of the studied compounds on changing the morphology of the cancer cell lines, and this behavior may be correlated to the high DNA binding affinity, this agrees well with the results of CT-DNA binding and the K_b values of the different coordination compounds (CuL = 5.16×10^5, CrL = 4.80×10^5 and FeL = 1.21×10^5).

4. Conclusion

Three new Cr(III), Fe(III) and Cu(II) coordination compounds

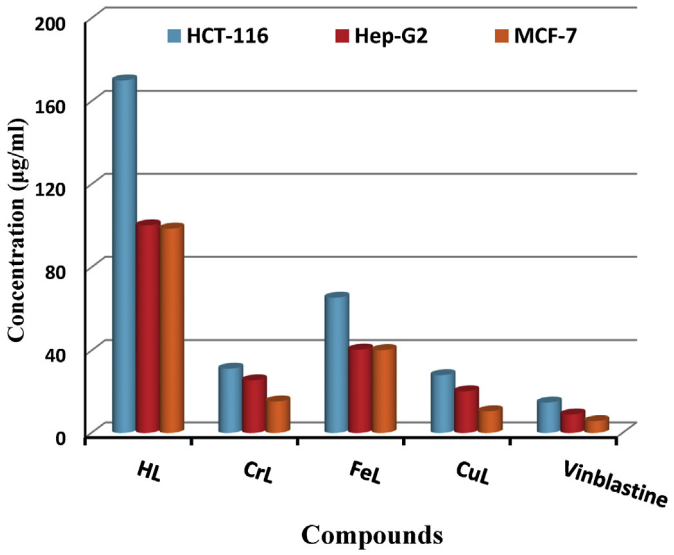

Fig. 6. The IC_{50} values of the aryl imidazole ligand HL, its coordination compounds and. vinblastine drug against HCT-116, Hep-G2 and MCF-7 cell lines.

have been synthesized and characterized *via* physicochemical, spectral analysis and DFT-calculations. The results showed that the ligand HL behaves as N, O - bidentate ligand and forms coordination compounds with Cr(III), Fe(III) and Cu(II) ions in a 1:1 M ratio. The studied coordination compounds are paramagnetic nature and have effective magnetic moment values. The Cr(III), Fe(III) and Cu(II) coordination compounds have a distorted-octahedral geometry as concluded from electronic and magnetic results and confirmed by the theoretical studies. The anti-pathogenic bioassay showed that the synthesized compounds are good antimicrobial medicines against the studied microorganisms as compared to used standard drugs. Moreover, the interactions of the titled coordination compounds with CT-DNA have been effectively estimated by electronic absorption, viscosity measurements, and gel electrophoresis methods. The DNA binding studies indicated that the interactions of the coordination compound with CT-DNA are intercalative modes. Furthermore, the growth inhibition effect of the prepared compounds was screened against HCT-116, HepG-2, and MCF-7 cell lines. Among these coordination compounds, CuL is more potent than CrL and FeL coordination compound. The biological results of our work would be useful in improving therapeutic drugs.

Acknowledgments

The authors thank Dr. ElSayed Shalaby (X-Ray Crystallography Lab, National Research Centre, El Behouth St., Dokki, Cairo, Egypt) for his help with x-ray data.

Appendix A. Supplementary data

CCDC 1943846 contains the supplementary crystallographic data for the prepared aryl imidazole ligand ($C_{25}H_{23}BrN_2O$). Material, instrumental and ^{1}Hnmr, ^{13}Cnmr and supplementary Figures and Table for IC_{50} values are given. Supplementary data to this article can be found online at https://doi.org/10.1016/j.molstruc.2019.127034.

References

[1] S. Das Sharma, P. Hazarika, D. Konwar, Tetrahedron Lett. 49 (2008) 2216.
[2] T. Prisinano, H. Law, M. Dukat, A. Slassi, N. MaClean, L. Demchyshyn, R.A. Glennon, Bioorg. Med. Chem. 9 (2001).
[3] S. Bhor, G. Anilkumar, M.K. Tse, M. Klawonn, C. Döbler, B. Bitterlich, A. Grotevendt, M. Beller, Org. Lett. 7 (2005) 3393.
[4] G.J. Lambardino, E.H. Wiseman, J. Med. Chem. 17 (1974) 1182.
[5] T. Maier, R. Schmierer, K. Bauer, H. Bieringer, H. Buerstell, B. Sachse, U.S. Patent 4820335, Chem. Abstr. 111 (1989) 19494w, 1989.
[6] S. Chowdhury, R.S. Mohan, J.L. Scott, Reactivity of ionicliquids, Tetrahedron 63 (2007) 2363.
[7] S. Chandra, R. Kumar, Transition Met. Chem. 29 (2004) 269.
[8] S. Chandra, R. Gupta, N. Gupta, S.S. Bawa, Transition Met. Chem. 31 (2006) 147.
[9] A. Katritzky R. Rees, Compr. Heterocycl. Chem. 5 (1984) 469.
[10] M. Grimmett, Ross, Imidazole and Benzimidazole Synthesis, Academic Press, 1997.
[11] E.G. Brown, Ring Nitrogen and Key Biomolecules, Kluwer Academic Press, 1998.
[12] A.F. Pozharskii, A.T. Soldatenkov, A.R. Katritzky, Heterocycles in Life and Society, John Wiley & Sons, 1997.
[13] T.L. Gilchrist, Heterocyclic Chemistry, the Bath press, 1985, ISBN 0-582-01421-2.
[14] J. Rajesh, M.P. Kesava, S. Ayyanaar, K. Karthikeyan, G. Rajagopal, P. Athappan, Appl. Organomet. Chem. 31 (2017) e3868. https://doi.org/10.1002/aoc.3868.
[15] A. Gubendran, G.G.V. Kumar, M.P. Kesavan, G. Rajagopal, P. Athappan, J. Rajesh, Appl. Organomet. Chem. 32 (2018) e4128. https://doi.org/10.1002/aoc.4128.
[16] A. Gubendran, M.P. Kesavan, S. Ayyanaar, L. Mitu, P. Athappan, J. Rajesh, Spectrochim. Acta A Mol. Biomol. Spectrosc. 181 (2017) 39–46.
[17] S.M. Kumar, M.P. Kesavan, G.G.V. Kumar, M. Sankarganesh, G. Chakkaravarthi, G. Rajagopal, J. Rajesh, J. Mol. Struct. 1153 (2018) 1–11.
[18] C.V. Rani, M.P. Kesavan, G.G.V. Kumar, M.J.D. Jeyaraj, J. Rajesh, G. Rajagopal, Appl. Organomet. Chem. 32 (2018) e4538. https://doi.org/10.1002/aoc.4538.
[19] J. Rajesh, M.P. Kesava, S. Ayyanaar, K. Karthikeyan, G. Rajagopal, P. Athappan, Appl. Organomet. Chem. 31 (2017) e3868. https://doi.org/10.1002/aoc.3868.
[20] L.H. Abdel-Rahman, A.M. Abu-Dief, M. Basha, A.A.H. Abdel-Mawgoud, Appl. Organomet. Chem. 31 (11) (2017), e3750. https://doi.org/10.1002/aoc.3750.
[21] L.H. Abdel-Rahman, A.M. Abu-Dief, M. Ismael, M.A.A. Mohamed, N.A. Hashem, J. Mol. Struct. 1103 (2016) 232.
[22] V.L. Borde, S.G. Shankarwar, C.D. Thakur, A.G. Shankarwar, Adv. Appl. Sci. Res. 5 (2014) 229.
[23] L.H. Abdel-Rahman, A.M. Abu-Dief, H. Moustafa, S.K. Hamdan, Appl. Organomet. Chem. 31 (2016) 3555.
[24] L.H. Abdel-Rahman, A.M. Abu-Dief, R.M. El-Khatib, S.M. Abdel-Fatah, Bioorg. Chem. 69 (2016) 140.
[25] S. Mackay, C.J. Gilmore, C. Edwards, N. Stewart, K. Shankl, maXus Computer Program for the Solution and Refinement of Crystal Structures. Bruker Nonius, MacScience, Japan & The University of Glasgow, The Netherlands, 1999.
[26] M. Tyagi, S. Chandra, J. Akhtar, D. Chand, J. Spectrochim. Acta A. 118 (2014) 1056.
[27] M.R. Hasan, M.A. Hossain, A.S. Md, M.N. Uddin, J. Taibah Univ. Sci. 10 (2016) 766.
[28] L.H. Abdel-Rahman, A.M. Abu-Dief, M.R. Shehata, F.M. Atlam, A.A.H. Abdel-Mawgoud, Appl. Organomet. Chem. 33 (2019) e4699. https://doi.org/10.1002/aoc.4699.
[29] L.H. Abdel-Rahman, A.M. Abu-Dief, H. Moustafa, A.A.H. Abdel-Mawgoud, Arab. J. Chem. (2017) in press, https://doi.org/10.1016/j.arabjc.2017.07.007.
[30] L.H. Abdel-Rahman, M.S.S. Adam, A.M. Abu-Dief, H. Moustafa, M.T. Basha, A.S. Aboraia, B.S. Al-Farhan, H.E. Ahmed, Appl. Organomet. Chem. 4527 (2018). https://doi.org/10.1002/aoc.4527.
[31] L.H. Abdel-Rahman, A.M. Abu-Dief, A.A. H Abdel-Mawgoud, J. King Saud Univ. Sci. 31 (1) (2019) 52–60.
[32] M.T. Basha, R.M. Alghanmi, M.R. Shehata, L.H. Abdel-Rahman, J. Mol. Struct. (2019), https://doi.org/10.1016/j.molstruc.2019.02.001.
[33] L.H. Abdel-Rahman, A.M. Abu-Dief, E.F. Newair, S.K. Hamdan, J. Photochem. Photobiol. B Biol. 160 (2016) 18.
[34] H.M. Abd El-Lateef, A.M. Abu-Dief, B.E.D.M. El-Gendy, J. Electroanal. Chem. 758 (2015) 135.
[35] H.M. Abd El-Lateef, A.M. Abu-Dief, L.H. Abdel-Rahman, E.C. Sañudo, N. Aliaga Alcalde, J. Electroanal. Chem. 743 (2015) 120.
[36] A.M. El-Saghier, H.F. Abd El-Halim, L.H. Abdel-Rahman, A. Kadry, Appl. Organometal. Chem. 33 (2019) 4641.
[37] B. Iftikhar, K. Javed, M.S.U. Khan, Z. Akhter, B. Mirza, V. Mckee, J. Mol. Struct. 1155 (2018) 337.
[38] D.M. Fouad, A. Bayoumi, M.A. El-Gahami, S.A. Ibrahim, A.M. Hammam, Nat. Sci. 2 (2010) 817.
[39] M. Gaber, M.K. Awad, F.M. Atlam, J. Mol. Struct. 1160 (2018) 348.
[40] G.G. Mohamed, E.M. Zayed, A.M.M. Hindy, Spectrochim. Acta A Mol. Biomol. Spectrosc. 145 (2015) 76.
[41] L.H. Abdel-Rahman, A.M. Abu-Dief, R.M. El-Khatib, S.M. Abdel-Fatah, A.A. Seleem, Inte. J. Nano. Chem. 2 (2016) 83.
[42] H.F. Abd El-halim, M.M. Omar, G.G. Mohamed, Spectrochim. Acta A. 78 (2011) 36.
[43] M.X. Li, L.Z. Zhang, C.L. Chen, J.Y. Niu, B.S. Ji, J. Inorg. Biochem. 106 (2012) 117.
[44] M.I. Abou-Dobara, N.F. Omar, M.A. Diab, A.Z. El-Sonbati, ShM. Morgan, M.A. El-Mogazy, J. Cell. Biochem. 120 (2019) 1667.
[45] P.G. Avajia, C.H.V. Kumarb, S.A. Patilc, K.N. Shivanandad, C. Nagaraju, Eur. J.

Med. Chem. 44 (2009) 3552.
[46] H.F.A. El-Halim, G.G. Mohamed, M.M.I. El-Dessouky, W.H. Mahmoud, Spectrochim. Acta A. 82 (2011) 8.
[47] H.W. Horowitz, G.M. Jetzger, Anal. Chem. 35 (1963) 1464.
[48] G.G. Mohamed, M.H. Soliman, Spectrochim. Acta A. 76 (2010) 341.
[49] A.N.M.A. Alaghaz, R.A. Ammar, Eur. J. Med. Chem. 45 (2010) 1314.
[50] F.S.M. Hassana, G.G. Mohamed, A.F. Al Hossainyc, M.A.S. Khidr, J. Pharm. Res. 5 (2012) 3753.
[51] L. Lekha, K. Kanmaniraja, G. Rajagopal, D. Sivakumar, D. Easwaramoorthi, Int. J. Chem. Pharm. Sci. 4 (2013) 48.
[52] P. Jayaseelan, E. Akila, M.U. Rani, R. Rajavel, Saudi j. Chem. Soc. 20 (2016) 625.
[53] MdS. Hossain, C.M. Zakaria, Md Kudrat-E-Zahan, Am. J. Heterocycl. Chem. 4 (2018) 1.
[54] M.A.A. Al-Soodani1, A.H.M. Ali, M.F. Al-Marjani, A.K. Atia, Int. J. Adv. Res. 2 (3) (2014) 399–408.
[55] M. Gomleksiz, C. Alkan, B. Erdem, S. Afr. J. Chem. 66 (2013) 107–112.
[56] I.N. Witwit1, Z.Y. Motaweq, H.M. MubarkJ, Pharm. Sci. Res. 10 (12) (2018) 3074–3083.
[57] M. Sunita, B. Anupama, B. Ushaiah, C.G. Kumari, Arab. J. Chem. 10 (2017) S3367.
[58] K. Savithri, B.C.V. Kumar, H.K. Vivek, H.D. Revanasiddappa, Int. J. Spectrosc. (2018). https://doi.org/10.1155/2018/8759372.
[59] M. Husain, G. Dehghan, A. Jouyban, P. Sistani, M. Arvin, Spectrochim. ActaA Mol. Biomol. Spectrosc. 120 (2014) 467.
[60] M.A. Husain, T. Sarwar, S.U. Rehman, H.M. Ishqi, M. Tabish, Physiol. Chem. Phys. 17 (2015) 13837.
[61] B.H. Alizadeh, Gh Dehghan, V.D. Ahmadi, S. Moghimi, A. Asadipour, A. Foroumadi, J. Sci. Islam. Repub. Iran 29 (2018) 121.
[62] S.S. Jawoor, S.A. Patil, S.S. Toragalmath, J. Coord. Chem. 71 (2018) 271. https://doi.org/10.1080/00958972.2017.1421951.
[63] E.I.M. El-Zahany, S.A. Drweesh, H.M. Awad, N.A. Hassan, M.M. Tarek, I. Potočňák, E. Int. Sci. Res. J. 72 (2016) 263.
[64] U. Sani, S.A. Dailami, Chem. Search J. 6 (2015) 35.
[65] B.G. Tweedy, Phytopatholoy 55 (1964) 910.
[66] L.M. Gaetke, C.K. Chow, Toxicology 189 (2003) 63.